Neural correlates of risky decision making in Parkinson's disease patients with impulse control disorders

Ruitenberg, M.F.L.; Koppelmans, V.; Wu, T.; Averbeck, B.B.; Chou, K.L.; Seidler, R.D.

Experimental Brain Research (2022) 240:2241–2253
https://doi.org/10.1007/s00221-022-06423-6

RESEARCH ARTICLE

Neural correlates of risky decision making in Parkinson's disease patients with impulse control disorders

Marit F. L. Ruitenberg[1,2] · Vincent Koppelmans[3] · Tina Wu[4] · Bruno B. Averbeck[5] · Kelvin L. Chou[6] · Rachael D. Seidler[7]

Received: 31 March 2022 / Accepted: 12 July 2022 / Published online: 19 July 2022

Abstract

Some patients with Parkinson's disease (PD) experience impulse control disorders (ICDs), characterized by deficient voluntary control over impulses, drives, or temptations regarding excessive hedonic behavior. The present study aimed to better understand the neural basis of impulsive, risky decision making in PD patients with ICDs by disentangling potential dysfunctions in decision and outcome mechanisms. We collected fMRI data from 20 patients with ICDs and 28 without ICDs performing an information gathering task. Patients viewed sequences of bead colors drawn from hidden urns and were instructed to infer the majority bead color in each urn. With each new bead, they could choose to either seek more evidence by drawing another bead (draw choice) or make an urn-inference (urn choice followed by feedback). We manipulated risk via the probability of bead color splits (80/20 vs. 60/40) and potential loss following an incorrect inference ($10 vs. $0). Patients also completed the Barratt Impulsiveness Scale (BIS) to assess impulsivity. Patients with ICDs showed greater urn choice-specific activation in the right middle frontal gyrus, overlapping the dorsal premotor cortex. Across all patients, fewer draw choices (i.e., more impulsivity) were associated with greater activation during both decision making and outcome processing in a variety of frontal and parietal areas, cerebellum, and bilateral striatum. Our findings demonstrate that ICDs in PD are associated with differences in neural processing of risk-related information and outcomes, implicating both reward and sensorimotor dopaminergic pathways.

Keywords Decision making · fMRI · Impulsivity · Parkinson's disease · Risk processing

Communicated by Hayley MacDonald.

Marit F. L. Ruitenberg and Vincent Koppelmans have contributed equally.

✉ Rachael D. Seidler
rachaelseidler@ufl.edu

1 Department of Health, Medical and Neuropsychology, Leiden University, Leiden, The Netherlands

2 Leiden Institute for Brain and Cognition, Leiden, The Netherlands

3 Department of Psychiatry, University of Utah, Salt Lake City, UT, USA

4 Department of Neurology, Cedars-Sinai Medical Center, Los Angeles, CA, USA

5 National Institute of Mental Health, Bethesda, MD, USA

6 Department of Neurology, University of Michigan Health System, Ann Arbor, MI, USA

7 Department of Applied Physiology and Kinesiology, University of Florida, 1864 Stadium Road, Gainesville, FL 32611, USA

Introduction

A subset of people with Parkinson's disease (PD) experience problems with impulse control, with prevalence estimates ranging from 20% (Weintraub and Claassen 2017) up to almost 45% (Monaco et al. 2018). Impulse control disorders (ICDs) refer to a set of behavioral disturbances in which a person lacks voluntary control over impulses, drives, or temptations to engage in excessive hedonic actions (Gatto and Aldinio 2019; Weintraub et al. 2006, 2015). The most common ICDs in PD are pathological gambling, hypersexual behavior, and compulsive buying or eating. Their development has been related to use of dopaminergic medication, in particular dopamine agonists (Ambermoon et al. 2011; Erga et al. 2017; Waskowiak et al. 2022; Weintraub et al. 2006, 2010).

Differences in brain structure and connectivity between patients with and without ICDs have been widely reported. For instance, morphological studies have shown reduced

gray matter volume and/or cortical thickness in the anterior cingulate cortex (ACC), orbitofrontal cortex (OFC), and striatum in patients with ICDs (e.g., Cerasa et al. 2014; Ruitenberg et al. 2018; Tessitore et al. 2016). Studies have further demonstrated that PD patients with ICDs showed decreased white matter structural connectivity in associative, limbic, and sensorimotor networks compared to those without (e.g., Canu et al. 2017; Imperiale et al. 2018; Mojtahed Zadeh et al. 2018). Notably, however, a recent systematic review concluded that the literature on both gray and white matter structural differences was inconsistent, and that the pathogenesis of ICDs in PD may rather be related to metabolic or functional alterations (Santangelo et al. 2019). Indeed, several studies have reported marked differences in resting state functional network connectivity between patients with and without ICDs (e.g., Carriere et al. 2015; Ruitenberg et al. 2018; Tessitore et al. 2017a, b), including weaker connectivity in an associative cortico-striatal network and the central executive network, and stronger connectivity in the salience network in PD patients with ICDs compared to those without. Furthermore, weaker frontal–striatal connectivity and stronger sensorimotor–striatal connectivity were associated with more impulsivity.

Less is known about the functional correlates of decision making and the processing of decision outcomes related to impulsive actions in PD patients with and without ICDs. Task-based fMRI studies found that during impulsive or risky responses (e.g., choosing between a sure vs. gamble option), PD patients with ICDs showed *less* activity within the ACC and OFC (Filip et al. 2018; Voon et al. 2011) and the ventral striatum (Rao et al. 2010; Politis et al. 2013; Voon et al. 2011; Girard et al. 2019) compared to patients without ICDs and controls. In contrast, during the processing of win outcomes they showed *more* activity in the OFC and ventral striatum (Frosini et al. 2010; Girard et al. 2019; Voon et al. 2010). Taken together, these findings suggest that PD patients with ICDs show alterations in affective, executive, and sensorimotor processing regions contributing to impulsive behaviors and the valuation of reward (for reviews, see Meyer et al. 2019; Santangelo et al. 2019).

While previous studies have elucidated the neural correlates of risk taking and reward processing in the context of ICDs in PD, they did not consider potential differences between patients with and without ICDs in terms of information gathering leading up to a decision. This is an important gap, because at the behavioral level PD patients with ICDs do not only urge for and engage in more risky behavior than patients without ICDs (e.g., Frosini et al. 2010; Voon et al. 2011), but they also have been reported to gather less information before making decisions (Djamshidian et al. 2012). Therefore, we investigated whether PD patients with ICDs may differently engage brain regions during each of the stages of risky decision making compared to patients without ICDs. We also examined whether brain activity during decision making was associated with individual differences in impulsive behaviors.

We had PD patients with and without ICDs perform an information gathering and decision making task in which they chose between evidence-seeking actions and actions leading to potential rewards or losses (Djamshidian et al. 2012; Furl and Averbeck 2011). Previous work in healthy participants demonstrated that those who gathered more information before decision making in this task engaged a parietal–frontal network more strongly compared to those who gathered less information (Furl and Averbeck 2011). The authors suggested that activation in the parietal cortex was associated with the amount of evidence-seeking chosen by the participant, while frontal areas were associated with weighing the value of making a risky decision. We hypothesized that compared to PD patients without ICDs, those with ICDs would show less frontal, parietal, and striatal activation during risky choices than during information gathering choices. We also explored potential group differences between choices under low vs. high certainty and loss conditions. We also hypothesized that PD patients with ICDs would assign more value to wins, and, therefore, would show stronger win vs. loss activation differences in the OFC and ventral striatum. Finally, we predicted that across all subjects more behavioral impulsivity would be associated with less ACC, OFC, and parietal activation during decision making and more activation in these regions during reward feedback processing.

Method

Participants

Participants in the present study overlapped with the same sample reported in Ruitenberg et al. (2018). They were recruited via the Fox Trial Finder from the Michael J. Fox Foundation for Parkinson's Research and through a collaborating physician's clinic (i.e., author KC). We classified 51 PD patients in the mild to moderate stages (aged 40–74 years, Hoehn and Yahr stages 1–3; Hoehn and Yahr 1967) as either having an ICD or not via the Questionnaire for Impulsive–Compulsive Disorders in Parkinson's disease (QUIP; Weintraub et al. 2009). In accordance with Weintraub et al. (2009), QUIP total scores from the first two sections (i.e., main ICDs and compulsive behaviors) were used to identify the presence or absence of an ICD (score 0 = no ICD, score 1 or higher = ICD).

The ICD+ group consisted of 21 patients who indicated pathologic gambling ($n = 1$), compulsive sexual behaviors ($n = 9$), compulsive buying ($n = 7$), compulsive eating ($n = 11$), or other compulsive behaviors ($n = 6$; nine

patients indicated a combination of two or more behaviors), whereas the ICD− group consisted of 30 patients indicating no such behaviors. All patients participated while their symptoms were being well-controlled by dopamine replacement medication. They provided written informed consent in accordance with the Declaration of Helsinki. The study was approved by the medical institutional review board of the University of Michigan.

Experimental task and procedure

Before performing the experimental task, patients completed several cognitive and clinical assessments. We used the Montreal Cognitive Assessment (MoCA; Nasreddine et al. 2005) and the National Adult Reading Test—Revised (NART-R; Blair and Spreen 1989) to assess patients' global cognitive abilities and verbal intelligence, respectively. We also used the Unified Parkinson's Disease Rating Scale (UPDRS) motor subscale to assess motor symptoms, and the Barratt Impulsiveness Scale questionnaire (BIS; Patton et al. 1995) to assess impulsiveness.

Patients then performed the "beads task", which has previously been used to investigate evidence seeking and impulsivity in healthy as well as clinical populations (e.g., Averbeck et al. 2011; Banca et al. 2016; Djamshidian et al. 2012; Furl and Averbeck 2011). Participants were instructed to imagine two urns filled with blue and green beads, with one (the "blue urn") containing mostly blue beads and the other (the "green urn") containing mostly green beads. On each trial, participants would view a sequence of beads drawn from one of the urns and their task was to infer from which urn each sequence of bead colors was drawn. At the start of each trial, an instruction screen showing the proportion of bead colors in the two urns (either 80/20 or 60/40 color split) and the cost for an incorrect urn inference (either \$10 or \$0) was presented. Participants then viewed a bead color followed by a response prompt, at which point they decided either to choose an urn or to draw another bead (maximum of nine draw choices per sequence). Depending on the participant's response the next stimulus was either a new bead color or a feedback screen showing whether the urn choice was (in)correct and how much money was won or lost during the trial. Participants completed six runs[1] of 16 bead sequences each, with four sequences per cell of a 2 × 2 design with bead probability (80/20 or 60/40) and loss (\$10 or \$0) as repeated measures factors such that all conditions occurred equally often.

[1] There were three patients who completed 5 runs, two who completed 4 runs, and one who completed 1 run of the task due to time limitations or other issues (e.g., feeling uncomfortable in the scanner).

Patients completed the task while lying supine in the scanner after having practiced the task outside of the scanner. Their responses were registered via an MRI-compatible claw with separate buttons designated for choosing the blue urn, the green urn, or drawing another bead. Prior to starting the task, structural and rs-fcMRI scans were obtained for each patient; results related to those data have been reported in Ruitenberg et al. (2018). The total duration of a test session was 90–120 min.

MRI acquisition

Structural and functional images were acquired on a 3 T GE Signa MRI scanner. For functional images we used a T2*-weighted gradient-echo pulse sequence. Across each run of the experimental task, the field of view (FOV) was 220 × 220 mm with a 64 × 64 × 43 matrix and 3 mm axial slice thickness (no slice gap) resulting in a voxel resolution of 3.44 × 3.44 × 3.00 mm (for two subjects the matrix was 64 × 64 × 35 and the voxel size was 3.44 × 3.44 × 3.50 mm). Repeat time to accomplish a full volume (TR) was 2000 ms, echo time (TE) was 30 ms, the flip angle was 90°, and all data were collected in an interleaved multi-slice mode. Prior to acquisition of the functional images, a structural scan was acquired using a T1-weighted spin-echo pulse sequence (TR = 540 ms, TE = 2.32 ms, flip angle = 15°) with a FOV of 220 × 220 mm and with a 256 × 256 × 124 matrix, resulting in an in-plane voxel resolution of 1.0156 × 1.0156 × 1.20 mm (scan duration ~ 10 min).

fMRI data processing

We excluded data from two subjects due to scanning artifacts (i.e., susceptibility artifacts), and data from one other subject due to technical problems. Data preprocessing was performed using fMRIPrep 1.3.0.post3 (Esteban et al. 2018, 2019), which is based on Nipype 1.1.9 (Gorgolewski et al. 2011, 2018). The following description of the fMRIprep pipeline is adapted from their standard methods transcript that is included with each subject report. For anatomical data preprocessing, the T1-weighted (T1w) image was corrected for intensity non-uniformity (INU) with N4BiasFieldCorrection (Tustison et al. 2010), distributed with ANTs 2.2.0 (Avants et al. 2008), and used as T1w-reference throughout the workflow. The T1w-reference was then skull-stripped using antsBrainExtraction.sh (ANTs 2.2.0), using OASIS30ANTs as the target template. Brain tissue segmentation of cerebrospinal fluid (CSF), white-matter (WM) and gray-matter (GM) was performed on the brain-extracted T1w using fast (FSL 5.0.9, Zhang et al. 2001).

For functional data preprocessing, the following preprocessing was performed for each of the two BOLD runs per subject (across all tasks and sessions). First, a reference

volume and its skull-stripped version were generated using a custom methodology of *fMRIPrep*. The BOLD reference was then co-registered to the T1w reference using bbregister (FreeSurfer) which implements boundary-based registration (Greve and Fischl 2009). Co-registration was configured with nine degrees of freedom to account for distortions remaining in the BOLD reference. Head-motion parameters with respect to the BOLD reference (transformation matrices, and six corresponding rotation and translation parameters) are estimated before any spatiotemporal filtering using mcflirt (FSL 5.0.9, Jenkinson et al. 2002). BOLD runs were slice-time corrected using 3dTshift from AFNI 20160207 (Cox and Hyde 1997). The BOLD time-series (including slice-timing correction when applied) were resampled onto their original, native space by applying a single, composite transform to correct for head-motion and susceptibility distortions. These resampled BOLD time-series will be referred to as *preprocessed BOLD in original space*, or just *preprocessed BOLD*. The BOLD time-series were resampled to MNI152NLin2009cAsym standard space, generating a *preprocessed BOLD run in MNI152NLin2009cAsym space*. First, a reference volume and its skull-stripped version were generated using a custom methodology of *fMRIPrep*. Several confounding time-series were calculated based on the *preprocessed BOLD*: framewise displacement (FD), temporal derivatives of variance over voxels (DVARS) and three regionwise global signals. FD and DVARS are calculated for each functional run, both using their implementations in *Nipype* (following the definitions by Power et al. 2014). The three global signals are extracted within the CSF, the WM, and the whole-brain masks. In addition, a set of physiological regressors were extracted to allow for component-based noise correction (*CompCor*, Behzadi et al. 2007). Principal components are estimated after high-pass filtering the *preprocessed BOLD* time-series (using a discrete cosine filter with 128 s cutoff) for the two *CompCor* variants: temporal (tCompCor) and anatomical (aCompCor). Six tCompCor components are then calculated from the top 5% variable voxels within a mask covering the subcortical regions. This subcortical mask is obtained by adaptively eroding the brain mask, which ensures it does not include cortical GM regions. For aCompCor, six components are calculated within the intersection of the aforementioned mask and the union of CSF and WM masks calculated in T1w space, after their projection to the native space of each functional run (using the inverse BOLD-to-T1w transformation). The head-motion estimates calculated in the correction step were also placed within the corresponding confounds file. We used a motion cutoff of 2 mm for framewise displacement, which was calculated as the sum of the absolute values of the differentiated 6 (3 translations and 3 rotations; rotations were converted to mm) realignment estimates (Power et al. 2012). Using this cutoff, the average proportion of outlier frames was 0.35% (range 0.06–4.01%); no subjects were excluded due to excessive head motion. Gridded (volumetric) resamplings were performed using antsApplyTransforms (ANTs), configured with Lanczos interpolation to minimize the smoothing effects of other kernels (Lanczos 1964). Finally, the data were smoothed with a 6 mm FWHM kernel.

fMRI analyses

We used SPM12 to perform our fMRI analyses. Data of all runs were detrended and combined into a single concatenated run to increase power to model infrequent events (e.g., if a participant made very few errors, so loss feedback was infrequent). Residual head motion and estimated physiological signals were regressed out by including six realignment parameters, five aCompCor components, and two tCompCor components during the first level contrast calculation. For the first-level analysis, we set up a contrast that examined the difference in brain activation between urn vs. draw choices. Two other contrasts examined activation differences between urn choices made in the high (80/20) and low (60/40) probability conditions and between those made in the \$10 and \$0 loss conditions. Second, we also set up contrasts that examined the difference between activation during win and loss feedback processing, as well as \$10 and \$0 loss feedback processing.

Second-level between-group and brain–behavior analyses were performed using Statistical Parametric Mapping software version 12 (SPM12; Wellcome Trust Center for Neuroimaging) running in the Matlab R2018b environment (Mathworks, Sherborn, MA, USA). We used non-parametric permutation tests with threshold free cluster enhancement (TFCE) controlled for the familywise error (FWE) rate ($p < 0.05$) for inference (TFCE Toolbox; Gaser 2019). We also report effects that were detected using an uncorrected statistical threshold of $p < 0.0005$, because group differences were expected to be somewhat subtle, given that the two groups both comprised people with Parkinson's disease and were comparable in terms of demographical and clinical features. We delineate in the tables and text when we are referring to corrected and uncorrected results. All analyses were conducted running 10,000 random permutations and included age as a covariate of no interest. First, we ran two-sample *t* tests to evaluate differences in brain activation between the ICD+ and ICD− patient groups. One contrast examined the group difference in activation between urn vs. draw choices. Two other contrasts examined group differences between 80/20 vs. 60/40 probability choices and between \$10 and \$0 loss choices. Second, we evaluated group differences related to feedback processing. Specifically, we ran a contrast to examine group differences in activation between win vs. loss feedback, as well as \$10 vs. \$0 loss feedback. Finally, we used one-sample *t* tests in

Table 1 Overview of the demographic and clinical characteristics of the ICD+ and ICD− groups (mean ± SD)

Measure	PD ICD+ ($n=20$)	PD ICD− ($n=28$)	Group difference
Age (years)	61 ± 5	62 ± 8	$t(46)=-0.29$, $p=.77$, $g=0.14$
Gender	7 F / 13 M	10 F / 18 M	$\chi^2(1)=0.03$, $p=.96$, $v=0.02$
Age of PD onset (years)[a]	55.9 ± 6.4	58.1 ± 8.5	$t(45)=-1.03$, $p=.31$, $g=0.29$
Disease duration (months)[a]	58.6 ± 30.9	44.2 ± 38.4	$t(45)=1.37$, $p=.18$, $g=0.41$
LED (mg)	587 ± 307	481 ± 331	$t(46)=1.13$, $p=.26$, $g=0.33$
UPDRS motor	25.95 ± 10.17	25.04 ± 9.76	$t(46)=0.31$, $p=.75$, $g=0.09$
BIS total score	61.60 ± 15.49	54.36 ± 8.95	***t*(46) = 2.05, *p* = .046, *g* = 0.60**
Attentional impulsiveness	16.00 ± 5.15	14.11 ± 3.51	$t(46)=1.52$, $p=.136$, $g=0.44$
Motor impulsiveness	21.90 ± 5.06	19.36 ± 2.84	***t*(46) = 2.22, *p* = .031, *g* = 0.65**
Non-planning impulsiveness	23.70 ± 6.56	20.89 ± 4.68	$t(46)=1.73$, $p=.090$, $g=0.51$
MoCA	27.90 ± 1.62	27.36 ± 1.57	$t(46)=1.16$, $p=.25$, $g=0.34$
NART-R (FSIQ score)	112.36 ± 7.74	112.40 ± 5.71	$t(46)=-0.20$, $p=.98$, $g=0.01$

PD, Parkinson's disease; BIS, Barratt Impulsiveness Scale; MoCA, Montreal Cognitive Assessment; NART-R, National Adult Reading Test—Revised; FSIQ, Full Scale IQ; LED, Levodopa Equivalent Dose; UPDRS, Unified Parkinson's Disease Rating Scale

[a]Data from one patient in the ICD− group were missing

which behavioral performance measures were entered as a covariate. This was done to search for brain regions in which activation was correlated with the average number of draw choices and with BIS scores, respectively. Note that we also ran one-sample *t* tests across all patients in our sample to verify whether brain areas involved in performance of the beads task were similar to those reported by Furl and Averbeck (2011); more details on these contrasts and corresponding results are reported in the Supplemental Materials.

We used the Harvard–Oxford Cortical and Subcortical Structural Atlases (Kennedy et al. 2016) for labeling cortical and subcortical areas, and the probabilistic cerebellar atlas (Diedrichsen et al. 2009) for labeling cerebellar areas.

Results

Group characteristics and behavioral results

Due to the aforementioned fMRI data exclusions, the final sample consisted of 20 patients in the ICD+ group and 28 patients in the ICD− groups. Table 1 presents the demographic and clinical characteristics of these groups. There were no significant differences in age, sex, disease duration, age of PD onset, UPDRS motor subscale scores, or levodopa equivalent dose between the groups ($ps > 0.19$). The ICD+ group scored significantly higher on the BIS questionnaire than the ICD− group, $t(46)=2.05$, $p=0.046$. MoCA scores ranged from 24 to 30 and did not differ significantly between the two patient groups ($p=0.25$). NART-R scores indicated that IQ estimates were within the normal range and did not differ significantly between groups ($p=0.98$).

We used the average number of draw choices per sequence and the proportion of correct urn choices as performance measures for the beads task (cf. Djamshidian et al. 2012; Furl and Averbeck 2011). For each measure, we performed a mixed ANOVA with Group (2; ICD+ vs. ICD−) as a between-subject variable and Probability (2; 80/20 vs. 60/40) and Loss (2; \$10 vs. \$0) as within-subject variables. Across all patients, we observed that more beads were drawn during sequences with 60/40 compared to 80/20 probability (2.61 vs. 1.54 draws), $F(1,46)=94.92$, $p<0.001$, $\eta_p^2=0.67$, and during \$10 loss than \$0 loss trials (2.30 vs. 1.85 draws), $F(1,46)=31.15$, $p<0.001$, $\eta_p^2=0.40$. In addition, patients more often chose the correct urn during sequences with 80/20 than 60/40 probability (0.88 vs. 0.72), $F(1,46)=108.19$, $p<0.001$, $\eta_p^2=0.70$. Finally, results showed a significant Probability × Loss interaction for correct urn choices, $F(1,46)=4.73$, $p=0.035$, $\eta_p^2=0.09$. Post hoc tests indicated that patients more often chose the correct urn when an incorrect choice would lead to \$10 compared to \$0 loss when the color split was 80/20 (\$10 = 0.90 vs. \$0 = 0.86), $F(1,46)=9.87$, $p=0.003$, $\eta_p^2=0.18$, but that potential loss did not affect accuracy when the color split was 60/40 (\$10 = 0.72 vs. \$0 = 0.73; $p=0.81$). Results showed no significant ICD group effects for either the number of drawn beads ($ps > 0.22$) or correct urn choices ($ps > 0.30$).

fMRI results

Group differences

Tables 2 and 3 summarize the TFCE and uncorrected results for the differences between the ICD+ and ICD− groups. For the Urn > Draw contrast, we observed

Table 2 Overview of the TFCE results for the second-level contrasts comparing activation in the ICD+ and ICD− groups. MFG = middle frontal gyrus

Group contrast	Anatomic location	Coordinates of peak	Cluster size (voxels)	$p_{FWE\text{-}corr}$
Urn > draw choices				
ICD+ > ICD–	R MFG	36, 16, 56	2	.049

greater activation differences between urn and draw choices in the ICD+ group compared to the ICD− group in the right middle frontal gyrus (Fig. 1). At the conservative uncorrected threshold, this activation difference was also detected. We further observed greater activation differences between urn and draw choices in the ICD+ group compared to the ICD− group in a variety of regions including the right middle frontal gyrus (in line with our TFCE result), lateral occipital gyrus, and cingulate gyrus, as well as bilateral temporal gyrus.

We found no other significant differences between the ICD+ and ICD− groups using the TFCE approach. At the uncorrected threshold, results further showed greater activation differences between urn choices under 80/20 vs. 60/40 probability in the ICD− compared to the ICD+ group in the cerebellum (Fig. 2a–c). During feedback processing, ICD+ patients showed a larger difference between win and loss activation compared to ICD− patients in the right frontal pole (Fig. 2d). No significant results were obtained at the uncorrected threshold for effects of loss condition ($10 vs. $0 loss) during urn choices or feedback processing.

Table 3 Overview of the uncorrected results for the second-level contrasts comparing activation in the ICD+ and ICD− groups

Group contrast	Anatomic location	Coordinates of peak	Cluster size (voxels)	*Z* score
Urn > draw choices				
ICD+ > ICD−	R MFG	36, 16, 56	138	4.81
	R MTG	64, − 27, − 15	59	4.63
	R LOC	48, − 69, 42	128	3.90
	L ITG	− 55, − 11, − 35	10	3.87
	R cingulate gyrus	2, − 43, 30	15	3.86
	R LOC	28, − 87, 18	16	3.83
	L FP	− 37, 54, − 13	17	3.78
	R LOC	22, − 81, 56	18	3.72
	L precuneus	− 1, − 57, 38	20	3.60
80/20 > 60/40 probability				
ICD− > ICD+	L CB lobule VI	− 5, − 67, − 13	10	4.11
	R CB lobule IX	4, − 57, − 43	10	3.96
	R CB crus II	18, − 71, − 39	11	3.61
Win > loss feedback				
ICD+ > ICD−	R FP	42, 48, 2	10	3.53

CB, cerebellum; FP, frontal pole; ITG, inferior temporal gyrus; LOC, lateral occipital cortex; MFG, middle frontal gyrus; MTG, middle temporal gyrus; OFC, orbitofrontal cortex

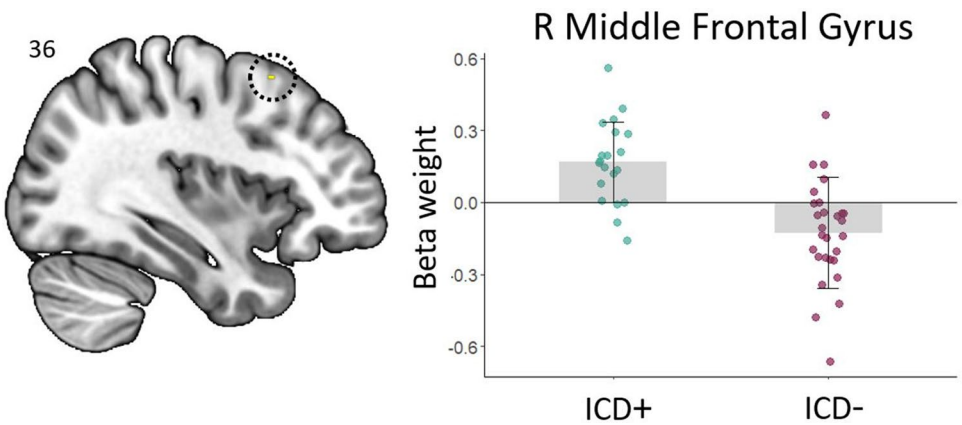

Fig. 1 Right middle frontal gyrus showing greater activation differences (TFCE approach) between urn and draw choices in the ICD+ as compared to the ICD− group

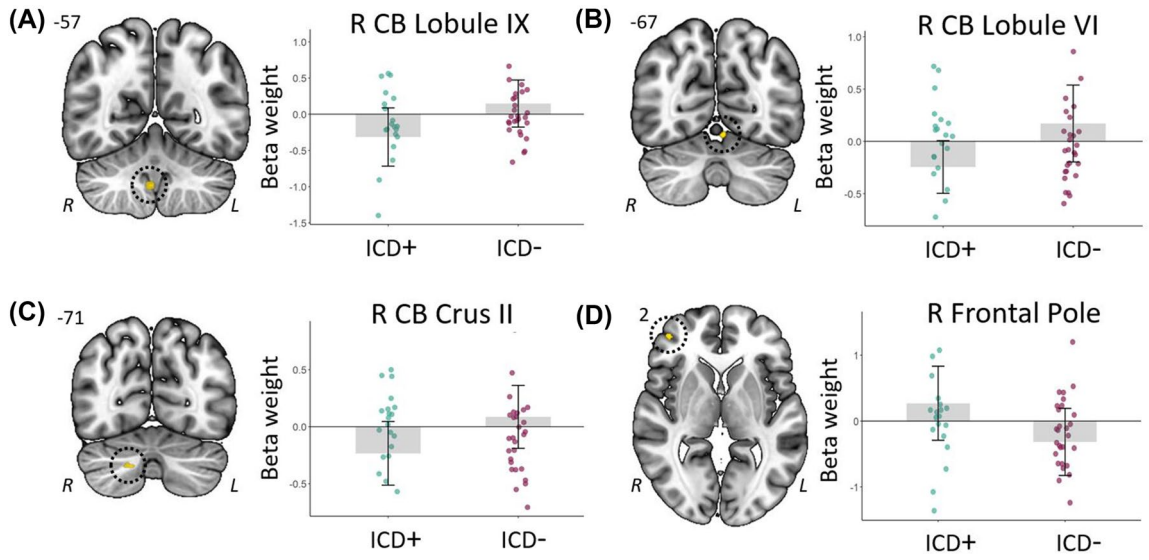

Fig. 2 **a**–**c** Cerebellar regions showing greater activation differences (uncorrected $p < .0005$) between urn choices under 80/20 and 60/40 probability in the ICD− as compared to the ICD+ group. **d** Right frontal pole showed greater activation differences (uncorrected $p < .0005$) between win and loss feedback in the ICD+ as compared to the ICD− group. For all panels, the right side of each image corresponds to the patients' left side

Table 4 Selected regions that show a correlation across patients between urn/win-specific activation and the number of draws in the beads task, using the TFCE approach

Index	Anatomic location	Direction	Coordinates of peak	Cluster size (voxels)	$p_{FWE\text{-}corr}$
Urn-specific activation					
# draws	R SMG	+	36, − 45, 40	31,171	< .001
	L lingual gyrus	+	− 5, − 19, 30	1029	.010
	L OFC	+	− 33, 28, − 1	365	.018
	R brain stem	+	4, − 35, − 3	13	.047
	L IFG	+	− 57, 20, − 5	13	.048
Win-specific activation					
# draws	R OP	−	12, − 101, 10	18,055	.002
	R precuneus	−	6, − 47, 56	6302	.009
	R preCG	−	64, 6, 22	300	.029
	R LOC	−	40, − 87, 36	52	.032
	L brain stem	−	− 11, − 27, − 11	97	.032
	R CB VIIIb	−	12, − 49, − 57	106	.033
	R thalamus / PHG	−	14, − 31, − 5	205	.034
	L planum temporale	−	− 57, − 23, 10	238	.035
	R SMG	−	64, − 23, 44	330	.037

Brain–behavior associations

Next, we identified brain regions showing a correlation across patients between urn-specific activation (urn > draw contrast) and individual differences in behavioral indices of impulsivity, namely, the number of draws in the beads task and scores on the BIS questionnaire. Using the TFCE approach, we only observed correlations for the number of draws in the beads task (Table 4). Specifically, greater urn-specific activation in a large cluster of frontal and parietal areas was associated with fewer draws (i.e., more impulsivity; Fig. 3). We did not observe any brain regions in which urn-specific activation was associated with BIS scores. At the conservative uncorrected threshold (Table 5), greater urn-specific activation in the right lingual gyrus was associated with fewer draws (i.e., more impulsivity). In contrast, greater activation in the right precentral, angular, and supramarginal gyri was associated

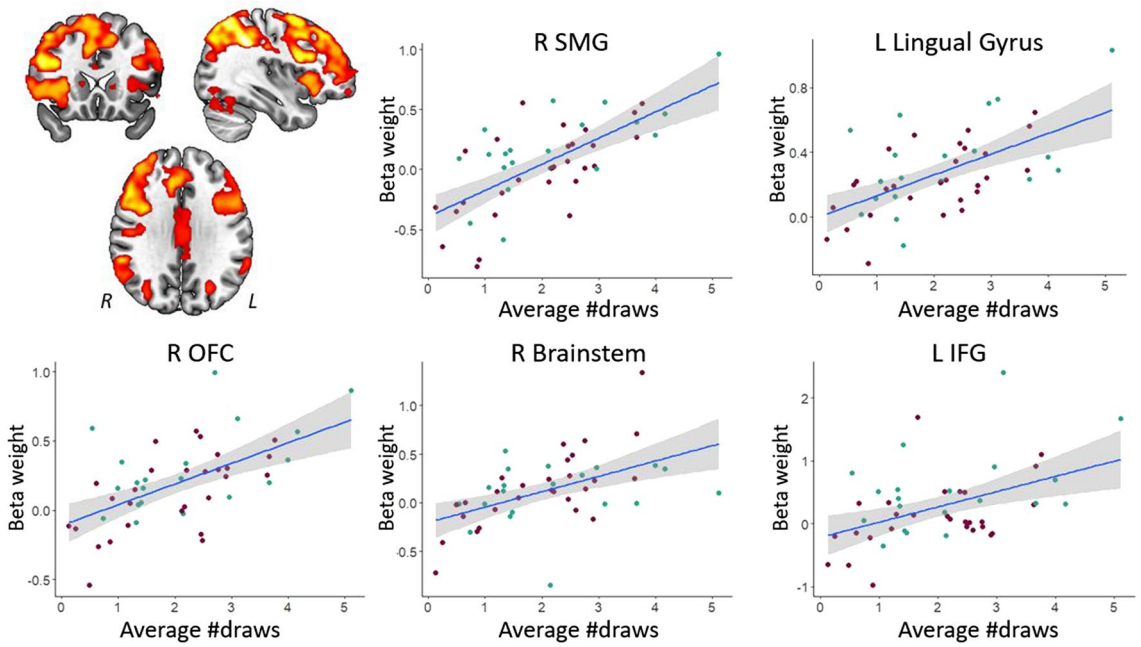

Fig. 3 Regions showing positive associations (at the TFCE level) between urn-specific activation and the number of draws. Note that *smaller* draw values reflect *more* impulsivity. The right side of the image corresponds to the patients' left side. The key for the abbreviations can be found in the notes of Table 4

Table 5 Regions that show a correlation across patients between urn/win-specific activation and behavioral indices of impulsivity (i.e., the number of draws in the beads task and scores on the BIS questionnaire), using the uncorrected threshold

Index	Anatomic location	Direction	Coordinates of peak	Cluster size (voxels)	*Z* score
Urn-specific activation					
# draws	R lingual gyrus	+	12, – 43, – 7	11	4.19
	R preCG	–	50, 10, 26	44	5.60
	R SMG	–	36, – 45, 40	74	5.46
	R angular gyrus	–	42, – 49, 48	(74)	5.34
	R SMG	–	48, – 35, 48	14	5.28
BIS scores	Brainstem	+	6, – 27, – 9	15	4.53
	R CB crus I	+	42, – 41, – 35	10	3.77
Win-specific activation					
# draws	L TMP [a]	+	– 43, 6, – 23	204	4.96
	R hippocampus	–	18,– 39, 4	10	3.79
	R temporal fusiform gyrus	–	36, – 15, – 33	17	3.70
	R PHG	–	30, – 21, – 25	18	3.62
	R cingulate gyrus	–	2, – 5, 24	17	3.79
BIS scores	R FP	+	36, 66, 18	15	3.66
	L precuneus	–	– 3, – 59, 58	69	4.66
	L SPL	–	– 29, – 41, 54	11	3.69

In the Direction column, + denotes that more impulsiveness was associated with greater activation, whereas – denotes that less impulsiveness was associated with greater activation. CB, cerebellum; FP, frontal pole; PHG, parahippocampal gyrus; preCG, precentral gyrus; SMG, supramarginal gyrus; SPL, superior parietal lobule; TMP, temporal pole

[a] Due to the very large number of observed areas, we only reported the area in which activation was significant at the FWE-corrected peak level

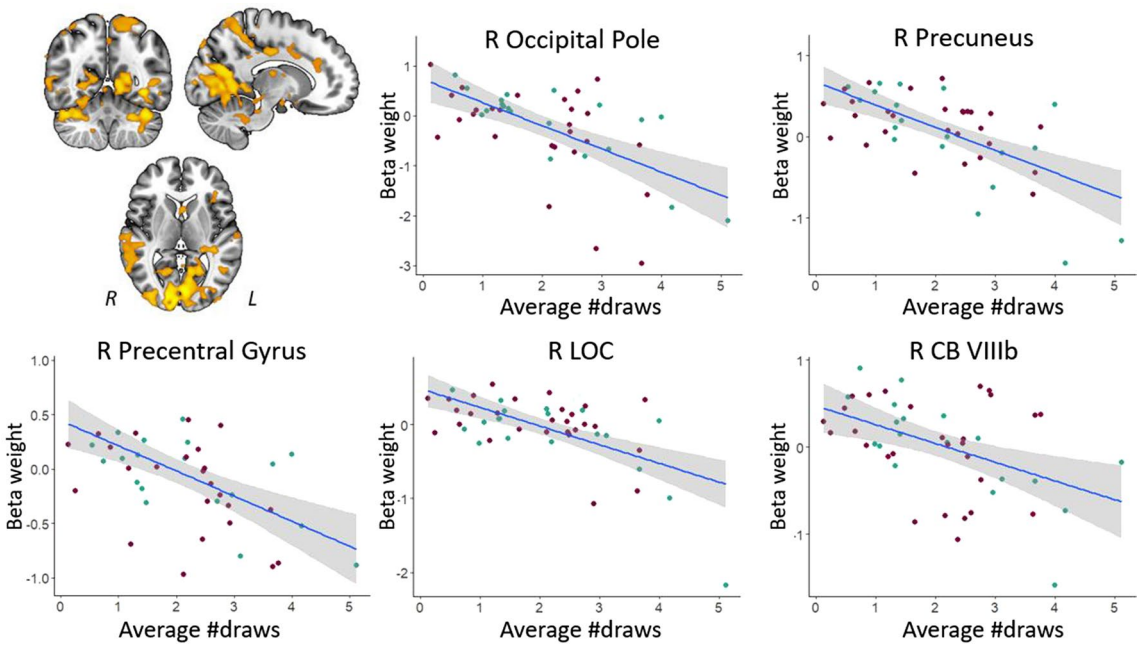

Fig. 4 Regions showing negative associations (at the TFCE level) between win-specific activation and the number of draws. Scatter plots illustrate the association between impulsiveness and activation for selected areas; note that *smaller* draw values reflect more impulsivity. The right side of each image corresponds to the patients' left side. The key for the abbreviations can be found in the notes of Table 4

with a higher number of draws (i.e., less impulsivity; Supplemental Figure 2a). For the BIS scores, greater urn-specific activation in the brain stem and right cerebellum was associated with more impulsivity (Supplemental Figure 2b). We did not observe any brain regions in which greater urn-specific activation was associated with lower BIS scores.

We also searched for brain regions showing a correlation across patients with individual differences in behavioral indices of impulsivity and win-specific activation (win > loss feedback contrast; Tables 4 and 5). Using the TFCE approach, results showed that greater win-specific activation in the primary motor cortex and a variety of parietal and occipital areas was associated with fewer draws (Fig. 4). Within the larger clusters, this association was also found for the bilateral calcarine cortex extending into the cerebellum, as well as for the bilateral striatum. At the conservative uncorrected threshold, greater win-specific activation in the temporal pole was associated with a smaller number of draws (i.e., more impulsivity; red regions in Supplemental Figure 3a), In contrast, greater activation in the cingulate gyrus and a variety of temporal areas including the hippocampus was associated with a higher number of draws (i.e., less impulsivity; blue regions in Supplemental Figure 3a). For the BIS scores, greater win-specific activation in the right frontal pole was associated with more impulsivity, whereas greater activation in the left precuneus and superior parietal lobule was associated with less impulsivity (Supplemental Figure 3b).

Discussion

The present study examined the neural basis of impulsive, risky decision making in PD patients, using a task-based fMRI approach. Below, we first discuss observed differences in brain activation during the information gathering task between PD patients with and without ICDs. We then discuss associations between individual differences in impulsivity and brain activation at the group level. Finally, we address the relationship between the present and previous findings within the context of dopaminergic networks that may contribute to impulsive behaviors and risky decision making in PD patients with ICDs.

We observed several differences in brain activation during various stages of the information gathering task between the two groups of PD. With regard to the behavioral choices following presentation of a new bead color, we found that patients with ICDs showed more activation during urn vs. draw choices in the right middle frontal gyrus, overlapping the dorsal premotor cortex, compared to those without. Furthermore, patients with ICDs showed a larger difference in activation between positive (win) and negative (loss) outcomes in the right frontal pole compared to ICD− patients.

As activation in this area has been linked to the processing of unexpected outcomes, both in terms of unexpected reward and unexpected absence of reward (Ramnani et al. 2004), our findings may indicate that patients with ICDs are poorer at making reward-related predictions. We further observed patients without ICDs showed larger probability-specific activation differences (i.e., 80/20 vs. 60/40 color split of the beads) in various cerebellar areas. In line with prior indications that the cerebellum is involved in uncertainty/probabilistic processing during decision making (Blackwood et al. 2004), this finding suggests that patients without ICDs take probability into account more during decision making compared to patients with ICDs. We observed no effects related to the amount of potential loss ($10 vs. $0), neither during decision making nor feedback processing. This may indicate that processing of the severity of prospective or actual loss does not significantly differ between patients with and without ICDs.

Across all patients in our study, we observed that less behavioral impulsivity (i.e., more draw choices) was associated with greater parietal activation during decision making. This is in line with observations in healthy adults, where urn-specific parietal activation was greater in individuals who sought more evidence and were less impulsive (Furl and Averbeck 2011). We further found that greater urn-specific activation in (pre)frontal regions including the OFC was associated with less impulsivity as reflected in more draw choices before selecting an urn. The OFC is known to be involved in evaluating choice values and causally related to subsequent decision making (Ballesta et al. 2020). Within the current paradigm, its involvement may reflect that individuals who more actively or efficiently evaluate urn vs. draw choice values show less behavioral impulsivity. Similarly, our observation that greater urn-specific activation in motor cortical areas and the striatum was associated with more draw choices may reflect that individuals who are better at distinguishing the two behavioral options at the neural level are less impulsive. Finally, results showed that greater win-specific activation in a variety of cortical and cerebellar motor areas and the thalamus during feedback processing was associated with more impulsivity (i.e., fewer draw choices). This may suggest that individuals who are more sensitive to reward also have a greater propensity to act in a more impulsive manner.

Our findings are in line with idea that differences in the mesolimbic dopamine reward system may underlie ICDs in patients with PD. As we additionally observed differences in a variety of cerebellar, striatal, and motor cortical areas, we believe that there are also sensorimotor components of impulsivity in PD. This parallels results from resting state functional connectivity and volumetric data we previously reported (Ruitenberg et al. 2018), and suggests that mesocortical and/or nigrostriatal dopamine pathways are also linked to impulsivity. To further explore this proposition, we performed post-hoc brain–behavior correlations between urn- and win-specific activation and scores on the motor impulsiveness subscale of the BIS. Results showed that greater activation in the right middle frontal gyrus, including the dorsal premotor cortex, as well as several sensory cortical areas was associated with more motor impulsivity (Supplemental Table 1). Taken together, our findings suggest that altered processing in these dopaminergic systems jointly contribute to impulsive behaviors in PD, rendering individuals to have both different affective and sensorimotor responses in the context of reward and risky decision-making. Admittedly, this interpretation is somewhat speculative as our study did not include a direct assessment of the dopamine system. Replication of the present work with the addition of novel techniques that can detect task-induced neurochemical changes and quantify dopamine transmission (e.g., functional PET or hybrid PET/fMRI; Ceccarini et al. 2020) will contribute to a more comprehensive understanding of the involvement of different dopaminergic pathways in ICDs. Future studies could further elucidate the neural basis of impulsivity in PD by evaluating potential differences among distinct ICD subtypes (e.g., compulsive gambling, hypersexuality, and punding), as these may have distinct pathophysiological bases (Voon et al. 2017).

A strength of the current study is that we used a large sample of patients relative to previous task-based fMRI studies on impulsivity in PD (i.e., ≥ 20 patients per group, compared to 7–14 patients per group in prior studies). In addition, the behavioral paradigm allowed us to examine the neural correlates of impulsivity in relation to evidence seeking, decision making, and outcome processing stages of risky behaviors. The observation that the pattern of results for the different task conditions in our patient sample is largely in line with those reported for healthy participants (Furl and Averbeck 2011) further supports that the task was implemented adequately and suitable for our clinical population. One may argue that the prevalence of ICD in our sample was relatively high, with 21 out of the 51 individuals with PD being classified as having an ICD. This may in part relate to the recruitment process during which the purpose of the study was described as investigating impulsivity in PD, which likely biased the sample. There are also some studies that report estimates of ICD prevalence in PD to be around 30–40% (e.g., 31% in Marin-Lahoz et al. 2018; 35% in Callesen et al. 2014; 44.7% in Monaco et al. 2018), which is close to what we see in our sample.

It could be argued that the lack of a healthy control group may be a limitation of the present work. In particular, this prevented us from evaluating any differences, at least from a behavioral point of view, between individuals with and without PD. However, given that we were interested in the neural basis of risky decision making in PD patients with

ICD compared to those without, rather than aberrant processing in PD or impulsivity in general, we consider the current design involving individuals with PD only to be appropriate. That is, we used a PD control group to compare against here. It should further be noted that all patients in our study were on dopamine replacement medication. While this may limit generalization of our findings as it does not allow us to consider any effect of medication status, it generally reflects the clinical status of PD patients as the vast majority of patients with ICDs are on medication. Moreover, the patient groups in our study did not differ in terms of levodopa equivalent dose, rendering it unlikely that it impacted our findings. Finally, studying patients while they are on dopamine replacement medication has two important practical benefits—it minimizes motor difficulties that patients in the off-medication state often experience which may confound performance, and it reduces potential movement-related artifacts during neuroimaging data collection.

Overall, our study demonstrates that ICDs in PD are associated with substantial differences in neural processing of risk-related information and outcomes, that implicate both affective and sensorimotor dopaminergic pathways. Understanding the underlying neural mechanisms of ICDs in PD could improve treatment strategies and provide biomarkers for tracking ICD risk and recovery. For example, our findings may provide a neurofunctional basis for developing targeted therapeutic interventions, as the cortical regions that we found to be differently recruited in patients with compared to those without ICDs could be potential target locations for interventions, such as noninvasive brain stimulation. With regard to the clinical significance of these results, it should be noted that the present study involved individuals that were screened positive for ICD but not necessarily clinically diagnosed with ICD. While our findings thus reveal cortical areas that could potentially be targeted in the treatment of ICDs, we recognize that replication in a group of individuals diagnosed with an ICD would be required before designing treatment with neurostimulation.

Conflict of interest

The authors declare that they have no conflict of interest.

Supplementary Information The online version contains supplementary material available at https://doi.org/10.1007/s00221-022-06423-6.

Acknowledgements We are grateful to the patients for their willingness to take part in this study. We thank the Fox Trial Finder from the Michael J. Fox Foundation for support with recruitment. This work was supported by the National Institute on Mental Health (ZIAMH002928-01 to BA) and the National Institute on Aging (1K01AG073578 to VK).

Funding National Institute of Mental Health, ZIAMH002928-01, Bruno B. Averbeck, National Institute on Aging, 1K01AG073578, Vincent Koppelmans

Data availability The data that support the findings of this study are available on request from the corresponding author.

References

Abraham A, Pedregosa F, Eickenberg M, Gervais P, Mueller A, Kossaifi J, Gramfort A, Thirion B, Varoquaux G (2014) Machine learning for neuroimaging with scikit-learn. Front Neuroinform 8:14

Ambermoon P, Carter A, Hall WD, Dissanayaka NN, O'Sullivan JD (2011) Impulse control disorders in patients with Parkinson's disease receiving dopamine replacement therapy: evidence and implications for the addictions field. Addiction 106:283–293

Avants BB, Epstein CL, Grossman M, Gee JC (2008) Symmetric diffeomorphic image registration with cross-correlation: evaluating automated labeling of elderly and neurodegenerative brain. Med Image Anal 12:26–41

Averbeck BB, Evans S, Chouhan V, Bristow E, Shergill SS (2011) Probabilistic learning and inference in schizophrenia. Schizophr Res 127:115–122

Ballesta S, Shi W, Conen KE, Padoa-Schioppa C (2020) Values encoded in orbitofrontal cortex are causally related to economic choices. Nature 588:450–453

Banca P, Lange I, Worbe Y, Howell NA, Irvine M, Harrison NA, Moutoussis M, Voon V (2016) Reflection impulsivity in binge drinking: behavioural and volumetric correlates. Addict Biol 21:504–515

Behzadi Y, Restom K, Liau J, Liu TT (2007) A component based noise correction method (CompCor) for BOLD and perfusion based fMRI. Neuroimage 37:90–101

Blackwood N, Simmons A, Bentall R, Murray R, Howard R (2004) The cerebellum and decision making under uncertainty. Cogn Brain Res 20:46–53

Blair JR, Spreen O (1989) Predicting premorbid IQ: a revision of the National Adult Reading Test. Clin Neuropsychol 3:129–136

Canu E, Agosta F, Markovic V, Petrovic I, Stankovic I, Imperiale F, Copetti M, Kostic VS, Filippi M (2017) White matter tract alterations in Parkinson's disease patients with punding. Parkinsonism Relat Disord 43:85–91

Carriere N, Lopes R, Defebvre L, Delmaire C, Dujardin K (2015) Impaired corticostriatal connectivity in impulse control disorders in Parkinson disease. Neurology 84:2116–2123

Ceccarini J, Liu H, Van Laere K, Morris ED, Sander CY (2020) Methods for quantifying neurotransmitter dynamics in the living brain with PET imaging. Front Physiol 11:792

Cerasa A, Salsone M, Nigro S, Chiriaco C, Donzuso G, Bosco D, Vasta R, Quattrone A (2014) Cortical volume and folding abnormalities in Parkinson's disease patients with pathological gambling. Parkinsonism Relat Disord 20:1209–1214

Cox RW, Hyde JS (1997) Software tools for analysis and visualization of fMRI data. NMR Biomed 10:171–178

Dale AM, Fischl B, Sereno MI (1999) Cortical surface-based analysis: I. Segmentation and surface reconstruction. Neuroimage 9(2):179–194

Diedrichsen J, Balster JH, Cussans E, Ramnani N (2009) A probabilistic MR atlas of the human cerebellum. Neuroimage 46:39–46

Djamshidian A, O'Sullivan SS, Sanotsky Y, Sharman S, Matviyenko Y, Foltynie T, Michalczuk R, Aviles-Olmos I, Fedoryshyn L, Doherty KM, Filts Y (2012) Decision making, impulsivity, and

addictions: do Parkinson's disease patients jump to conclusions? Mov Disord 27:1137–1145
Erga AH, Alves G, Larsen JP, Tysnes OB, Pedersen KF (2017) Impulsive and compulsive behaviors in Parkinson's disease: the Norwegian ParkWest study. J Parkinson's Dis 7:183–191
Esteban O, Blair R, Markiewicz CJ, Berleant SL, Moodie C, Ma F, Grogolewski KJ (2018) fMRIPrep. 10.5281/zenodo.852659
Esteban O, Markiewicz CJ, Blair RW, Moodie CA, Isik AI, Erramuzpe A, Kent JD, Goncalves M, DuPre E, Snyder M, Oya H (2019) fMRIPrep: a robust preprocessing pipeline for functional MRI. Nat Methods 16:111–116
Filip P, Linhartová P, Hlavatá P, Šumec R, Baláž M, Bareš M, Kašpárek T (2018) Disruption of multiple distinctive neural networks associated with impulse control disorder in Parkinson's disease. Front Hum Neurosci 12:462
Fonov VS, Evans AC, McKinstry RC, Almli CR, Collins DL (2009) Unbiased nonlinear average age-appropriate brain templates from birth to adulthood. Neuroimage 47:S102
Frosini D, Pesaresi I, Cosottini M, Belmonte G, Rossi C, Dell'Osso L, Murri L, Bonuccelli U, Ceravolo R (2010) Parkinson's disease and pathological gambling: results from a functional MRI study. Mov Disord 25:2449–2453
Furl N, Averbeck BB (2011) Parietal cortex and insula relate to evidence seeking relevant to reward-related decisions. J Neurosci 31:17572–17582
Gaser C (2019). Threshold-free cluster enhancement toolbox. https://doi.org/10.5281/zenodo.2641381
Gatto EM, Aldinio V (2019) Impulse control disorders in Parkinson's disease. A brief and comprehensive review. Front Neurol 10:351
Girard R, Obeso I, Thobois S, Park SA, Vidal T, Favre E, Ulla M, Broussolle E, Krack P, Durif F, Dreher JC (2019) Wait and you shall see: sexual delay discounting in hypersexual Parkinson's disease. Brain 142:146–162
Gorgolewski K, Burns CD, Madison C, Clark D, Halchenko YO, Waskom ML, Ghosh SS (2011) Nipype: a flexible, lightweight and extensible neuroimaging data processing framework in python. Front Neuroinform 5:13
Gorgolewski KJ, Esteban O, Markiewicz CJ, Ziegler E, Ellis DG, Notter MP et al (2018) Nipype. https://nipype.readthedocs.io/en/0.12.0/index.html
Greve DN, Fischl B (2009) Accurate and robust brain image alignment using boundary-based registration. Neuroimage 48:63–72
Hoehn MM, Yahr MD (1967) Parkinsonism: onset, progression, and mortality. Neurology 17:427–442
Imperiale F, Agosta F, Canu E, Markovic V, Inuggi A, Jecmenica-Lukic M, Tomic A, Copetti M, Basaia S, Kostic VS, Filippi M (2018) Brain structural and functional signatures of impulsive–compulsive behaviours in Parkinson's disease. Mol Psychiatry 23:459–466
Jenkinson M, Bannister P, Brady M, Smith S (2002) Improved optimization for the robust and accurate linear registration and motion correction of brain images. Neuroimage 17:825–841
Kennedy D, Haselgrove C, Fischl B, Breeze J, Frazier J, Seidman L, Goldstein J, Kosofsky B (2016) Harvard Oxford cortical and subcortical structural atlases. Harvard Center for Morphometric Analysis, Boston, MA
Klein A, Ghosh SS, Bao FS, Giard J, Häme Y, Stavsky E, Lee N, Rossa B, Reuter M, Chaibub Neto E, Keshavan A (2017) Mindboggling morphometry of human brains. PLoS Comput Biol 13:e1005350
Lanczos C (1964) Evaluation of noisy data. J Soc Ind Appl Math Ser B Numer Anal 1:76–85
Meyer GM, Spay C, Laurencin C, Ballanger B, Sescousse G, Boulinguez P (2019) Functional imaging studies of impulse control disorders in Parkinson's disease need a stronger neurocognitive footing. Neurosci Biobehav Rev 98:164–176
Mojtahed Zadeh M, Ashraf-Ganjouei A, Ghazi Sherbaf F, Haghshomar M, Aarabi MH (2018) White matter tract alterations in drug-naïve Parkinson's disease patients with impulse control disorders. Front Neurol 9:163
Nasreddine ZS, Phillips NA, Bédirian V, Charbonneau S, Whitehead V, Collin I, Cummings JL, Chertkow H (2005) The montreal cognitive assessment, MoCA: a brief screening tool for mild cognitive impairment. J Am Geriatr Soc 53:695–699
Patton JH, Stanford MS, Barratt ES (1995) Factor structure of the Barratt impulsiveness scale. J Clin Psychol 51:768–774
Politis M, Loane C, Wu K, O'Sullivan SS, Woodhead Z, Kiferle L, Lawrence AD, Lees AJ, Piccini P (2013) Neural response to visual sexual cues in dopamine treatment-linked hypersexuality in Parkinson's disease. Brain 136:400–411
Power JD, Barnes KA, Snyder AZ, Schlaggar BL, Petersen SE (2012) Spurious but systematic correlations in functional connectivity MRI networks arise from subject motion. Neuroimage 59:2142–2154
Power JD, Mitra A, Laumann TO, Snyder AZ, Schlaggar BL, Petersen SE (2014) Methods to detect, characterize, and remove motion artifact in resting state fMRI. Neuroimage 84:320–341
Ramnani N, Elliott R, Athwal BS, Passingham RE (2004) Prediction error for free monetary reward in the human prefrontal cortex. Neuroimage 23:777–786
Rao H, Mamikonyan E, Detre JA, Siderowf AD, Stern MB, Potenza MN, Weintraub D (2010) Decreased ventral striatal activity with impulse control disorders in Parkinson's disease. Mov Disord 25:1660–1669
Ruitenberg MFL, Wu T, Chou KL, Koppelmans V, Averbeck BB, Seidler RD (2018) Impulsivity in Parkinson's disease is associated with alterations in affective and sensorimotor striatal networks. Front Neurol 9:279
Santangelo G, Raimo S, Cropano M, Vitale C, Barone P, Trojano L (2019) Neural bases of impulse control disorders in Parkinson's disease: a systematic review and an ALE meta-analysis. Neurosci Biobehav Rev 107:672–685
Tessitore A, De Micco R, Giordano A, di Nardo F, Caiazzo G, Siciliano M, De Stefano M, Russo A, Esposito F, Tedeschi G (2017a) Intrinsic brain connectivity predicts impulse control disorders in patients with Parkinson's disease. Mov Disord 32:1710–1719
Tessitore A, Santangelo G, De Micco R, Giordano A, Raimo S, Amboni M, Esposito F, Barone P, Tedeschi G, Vitale C (2017b) Resting-state brain networks in patients with Parkinson's disease and impulse control disorders. Cortex 94:63–72
Tessitore A, Santangelo G, De Micco R, Vitale C, Giordano A, Raimo S, Corbo D, Amboni M, Barone P, Tedeschi G (2016) Cortical thickness changes in patients with Parkinson's disease and impulse control disorders. Parkinsonism Relat Disord 24:119–125
Tustison NJ, Avants BB, Cook PA, Zheng Y, Egan A, Yushkevich PA, Gee JC (2010) N4ITK: improved N3 bias correction. IEEE Trans Med Imaging 29:1310–1320
Voon V, Gao J, Brezing C, Symmonds M, Ekanayake V, Fernandez H, Dolan RJ, Hallett M (2011) Dopamine agonists and risk: impulse control disorders in Parkinson's disease. Brain 134:1438–1446
Voon V, Napier TC, Frank MJ, Sgambato-Faure V, Grace AA, Rodriguez-Oroz M, Obseso J, Bezard E, Fernagut P-O (2017) Impulse control disorders and levodopa-induced dyskinesias in Parkinson's disease: an update. Lancet Neurol 16:238–250
Voon V, Pessiglione M, Brezing C, Gallea C, Fernandez HH, Dolan RJ, Hallett M (2010) Mechanisms underlying dopamine-mediated reward bias in compulsive behaviors. Neuron 65:135–142
Waskowiak P, Koppelmans V, Ruitenberg MFL (2022) Trait anxiety as a risk factor for impulse control disorders in Parkinson's disease. J Parkinson's Dis 12:689–697
Weintraub D, Claassen DO (2017) Impulse control and related disorders in Parkinson's disease. Int Rev Neurobiol 133:679–717

Weintraub D, David AS, Evans AH, Grant JE, Stacy M (2015) Clinical spectrum of impulse control disorders in Parkinson's disease. Mov Disord 30:121–127

Weintraub D, Hoops S, Shea JA, Lyons KE, Pahwa R, Driver-Dunckley ED, Adler CH, Potenza MN, Miyasaki J, Siderowf AD, Voon V (2009) Validation of the questionnaire for impulsive-compulsive disorders in Parkinson's disease. Mov Disord 24:1461–1467

Weintraub D, Koester J, Potenza MN, Siderowf AD, Stacy M, Voon V, Whetteckey J, Wunderlich GR, Lang AE (2010) Impulse control disorders in Parkinson disease: a cross-sectional study of 3090 patients. Arch Neurol 67:589–595

Weintraub D, Siderowf AD, Potenza MN, Goveas J, Morales KH, Duda JE, Moberg PJ, Stern MB (2006) Association of dopamine agonist use with impulse control disorders in Parkinson disease. Arch Neurol 63:969–973

Zhang Y, Brady M, Smith S (2001) Segmentation of brain MR images through a hidden Markov random field model and the expectation-maximization algorithm. IEEE Trans Med Imaging 20:45–57